# Noise Removal for Dynamic Mode Decomposition Based on Plug-and-Play ADMM

Shunki Anami* and Ryo Matsuoka†
* The University of Kitakyushu, Fukuoka, Japan
E-mail: c1mca004@eng.kitakyu-u.ac.jp
† The University of Kitakyushu, Fukuoka, Japan
E-mail: r-matsuoka@kitakyu-u.ac.jp

***Abstract*—Dynamic mode decomposition (DMD) is useful for video background/foreground separation. This decomposition algorithm can decompose a video into a set of dynamic modes, called the DMD mode, and then separate the near-zero mode as the stationary background and the other modes as the moving foreground components. However, When foreground/background separation is performed on noisy video, noisy background/foreground components are obtained because the DMD mode is degraded by noise. This paper proposes a novel noise removal method for the DMD mode of a noisy video. Specifically, we formulate a minimization problem that simultaneously reduces the noise of the DMD mode and the reconstructed video. The proposed minimization problem is solved by an algorithm based on Plug-and-Play alternating direction method of multipliers (PnP-ADMM). The experimental results demonstrate the advantages of the proposed method compared with a conventional noise removal method.**

## I. Introduction

In surveillance and in-vehicle systems, video processing such as noise removal, foreground/background separation, and object detection is important. Background/foreground separation is generally an essential step in the detection, identification, tracking, and recognition of objects in a video sequence. Dynamic mode decomposition (DMD) is often used for background/foreground separation [1]–[5]. DMD has introduced in the field of fluid dynamics and emerged as a powerful tool for analyzing the dynamics of nonlinear systems [6]–[8]. In background/foreground separation, the DMD method identifies a static background by performing a temporal Fourier decomposition of video frames. Specifically, it separates a stationary background and a dynamic foreground by distinguishing between modes close to zero and the remaining modes.

High-sensitivity shooting in a low-light condition increases sensor noise, resulting in a noisy video. When foreground/background separation based on DMD is performed on such noisy data, noisy background/foreground components, which are not suitable for video analysis, are obtained. This is because the DMD mode is seriously degraded by noise. In the case of fluid analysis, the total-DMD (TDMD) algorithm based on total least-squares has been proposed to reduce the bias error caused by sensor noise [9], [10]. When TDMD-based methods are applied to the foreground-background separation problem, they cannot sufficiently remove the spatial noise because they do not take into account the prior-knowledge that promotes image smoothness.

For image/video noise removal, optimization-based methods such as total variation regularization [11]–[14] and filtering-based denoising methods such as BM3D [15] have been proposed. These methods can remove noise by promoting spatial smoothness. However, in order to intelligently remove noise from the noisy video, we need to consider the consistency of the time direction. Existing methods that only consider spatial smoothness will result in artifacts such as flickering and pseudo-edges when played back as video. Furthermore, a method to directly remove the noise of the DMD mode, which is obtained by decomposing noisy video, has not been investigated.

In this paper, we propose a novel noise removal method for the DMD mode of a noisy video. Specifically, we formulate a minimization problem based on the Plug-and-Play framework that simultaneously reduces the noise of the DMD mode and the reconstructed video. Furthermore, we introduce an algorithm based on the Plug-and-Play alternating direction method of multipliers (PnP-ADMM) to solve the proposed minimization problem. Experimental results show the effectiveness of the proposed method by comparing with a conventional noise removal method.

The paper is organized as follows. In Section II, we present mathematical preliminaries, a DMD algorithm, and a PnP-ADMM algorithm. Section III introduces a novel minimization problem for DMD mode denoising. In Section IV, several examples are presented and compared with a conventional denoising method to verify the effectiveness of the proposed method. Finally, we conclude this paper in Section V.

## II. Preliminaries

Throughout this paper, bold-faced lowercase and uppercase letters indicate vectors and matrices, respectively. Real- and complex-valued $N$-dimensional vector spaces denote by $\mathbb{R}^N$ and $\mathbb{C}^N$, respectively. We define the set of $N \times M$ real-valued and complex-valued matrices as $\mathbb{R}^{N\times M}$ and $\mathbb{C}^{N\times M}$, respectively. The operations of nonconjugate and conjugate transpose of vectors and matrices are denoted as $(\cdot)^\top$ and $(\cdot)^*$, respectively. The operation of extracting the diagonal components of a diagonal matrix $\mathbf{X}$ and converting it into a column vector is defined by $\mathrm{diag}(\mathbf{X})$.

### A. Dynamic Mode Decomposition

The DMD algorithm is defined for pairs of data $\{\mathbf{x}_i, \mathbf{y}_i\}$ satisfying $\mathbf{y}_i = \mathbf{A}\mathbf{x}_i \quad (i = 1, \ldots, M)$, for some matrix $\mathbf{A}$. These vectors are sampled by equispaced snapshots of some dynamical system. However, the matrix $\mathbf{A}$ is not completely determined by the snapshots in most cases. The DMD algorithm estimates $\mathbf{A}$ such that satisfying $\mathbf{Y} \approx \mathbf{A}\mathbf{X}$, where $\mathbf{Y} := [\mathbf{y}_1, \ldots, \mathbf{y}_M]$ and $\mathbf{X} := [\mathbf{x}_1, \ldots, \mathbf{x}_M]$. Several methods have been proposed to calculate DMD [6], [9], [10], [16], [17]. In this paper, we use the basic DMD algorithm [6].

The DMD algorithm [6] is described as follows:

(i) Calculate the (reduced) *singular value decomposition* (SVD) of the matrix $\mathbf{X}$ as $\mathbf{X} = \mathbf{U}\mathbf{S}\mathbf{V}^*$, where $\mathbf{U} \in \mathbb{C}^{N\times r}$, $\mathbf{S} \in \mathbb{C}^{r\times r}$, and $\mathbf{V} \in \mathbb{C}^{M\times r}$, with the rank $r$.

(ii) Let $\tilde{\mathbf{A}}$ be defined by $\tilde{\mathbf{A}} = \mathbf{U}^*\mathbf{Y}\mathbf{V}\mathbf{S}^{-1}$.

(iii) Compute the eigendecomposition of $\tilde{\mathbf{A}}$ as $\tilde{\mathbf{A}}\mathbf{W} = \mathbf{W}\mathbf{\Lambda}$, where $\mathbf{W} := [\mathbf{w}_1, \ldots, \mathbf{w}_r]$ is a matrix that is configured by arranging the eigenvectors $\mathbf{w}_i \in \mathbb{C}^r \ (i = 1, \ldots, r)$ and $\mathbf{\Lambda}$ is a diagonal matrix having eigenvalues $\lambda_i \ (i = 1, \ldots, r)$ as the diagonal elements.

(iv) The DMD mode $\mathbf{\Phi} := [\phi_1, \ldots, \phi_r] \ (\phi_i \in \mathbb{C}^N)$ is obtained by $\mathbf{\Phi} = \mathbf{U}\mathbf{W}$.

(v) Then, we define $\mathbf{\Sigma} \in \mathbb{C}^{r\times M}$ as

$$\mathbf{\Sigma} := [\mathrm{diag}(\mathbf{\Lambda}^0)\ \mathrm{diag}(\mathbf{\Lambda}^1)\ \cdots\ \mathrm{diag}(\mathbf{\Lambda}^{M-1})]. \tag{1}$$

(vi) Estimate the diagonal matrix $\mathbf{B} \in \mathbb{C}^{r\times r}$ by minimizing the cost function

$$E(\mathbf{B}) := \|\mathbf{X} - \mathbf{\Phi}\mathbf{B}\mathbf{\Sigma}\|_F^2. \tag{2}$$

(vii) Finally, $\mathbf{X}$ is decomposed by $\mathbf{\Phi}, \mathbf{B}$, and $\mathbf{\Sigma}$ as

$$\mathbf{X} \approx \mathbf{\Phi}\mathbf{B}\mathbf{\Sigma}. \tag{3}$$

In this manner, the DMD algorithm decomposes $\mathbf{X}$ into $\mathbf{\Phi}, \mathbf{B}$, and $\mathbf{\Sigma}$, where $\mathbf{\Phi}$ is the set of dynamic modes of observed dynamical systems, each diagonal element of $\mathbf{B}$ is the amplitude of each mode, and each row of $\mathbf{\Sigma}$ is a Vandermonde matrix describing the temporal evolution of each mode.

### B. Plug-and-Play Alternating Direction Method of Multipliers

Alternating direction method of multipliers (ADMM) [18] is a proximal splitting algorithm that can treat convex optimization problems of the form

$$\min_{\mathbf{x}\in\mathbb{R}^{N_1},\, \mathbf{z}\in\mathbb{R}^{N_2}} F(\mathbf{x}) + G(\mathbf{z}) \ \text{ s.t. } \ \mathbf{z} = \mathbf{L}\mathbf{x}, \tag{4}$$

where $F$ and $G$ are usually assumed to be a quadratic and proximable function, respectively, and $\mathbf{L} \in \mathbb{R}^{N_2\times N_1}$ is a matrix with full-column rank. For any $\mathbf{x}^{(0)} \in \mathbb{R}^{N_1}, \mathbf{z}^{(0)} \in \mathbb{R}^{N_2}, \mathbf{b}^{(0)} \in \mathbb{R}^{N_2}$ and $\gamma > 0$, the ADMM algorithm is given by

$$\left\lfloor \begin{array}{l} \mathbf{x}^{(t+1)} = \arg\min_{\mathbf{x}} \left\{F(\mathbf{x}) + \frac{\gamma}{2}\|\mathbf{z}^{(t)} - \mathbf{L}\mathbf{x} - \mathbf{b}^{(t)}\|_2^2\right\}, \\ \mathbf{z}^{(t+1)} = \arg\min_{\mathbf{z}} \left\{G(\mathbf{z}) + \frac{\gamma}{2}\|\mathbf{z} - \mathbf{L}\mathbf{x}^{(t+1)} - \mathbf{b}^{(t)}\|_2^2\right\}, \\ \mathbf{b}^{(t+1)} = \mathbf{b}^{(t)} + \mathbf{L}\mathbf{x}^{(t+1)} - \mathbf{z}^{(t+1)}, \end{array}\right. \tag{5}$$

where the superscript $(t)$ denotes the iteration number. The sequence generated by (5) quickly converges to an optimal solution of (4).

In PnP-ADMM [19], [20], the solution of the sub-problem w.r.t. $\mathbf{z}$ is replaced by an off-the-shelf denoising algorithm, to yield

$$\mathbf{z}^{(t+1)} = \mathcal{D}_\sigma\left(\mathbf{x}^{(t+1)} + \mathbf{b}^{(t)}\right), \tag{6}$$

where $\mathcal{D}_\sigma$ denotes the Gaussian denoiser and $\sigma$ is the standard deviation of the assumed additive white Gaussian noise (AWGN).

*1) Ball Constraint:* The $\mathbf{v}$ centered $\ell_2$-norm ball with radius $\epsilon > 0$ is adopted as data-fidelity, implying that $F$ of (4) equals to the indicator function[1] of the ball, i.e., $F(\mathbf{x}) := \iota_{\mathcal{B}^2_{\mathbf{v},\epsilon}}(\mathbf{x})$ with $\mathcal{B}^2_{\mathbf{v},\epsilon} := \{\mathbf{x} \mid \|\mathbf{x} - \mathbf{v}\|_2 \leq \epsilon\}$. The minimization problem $\min_{\mathbf{y}} \iota_{\mathcal{B}^2_{\mathbf{v},\epsilon}}(\mathbf{y}) + \frac{1}{2\gamma}\|\mathbf{x} - \mathbf{y}\|_2^2$ equals to the metric projection onto $\mathcal{B}^2_{\mathbf{v},\epsilon}$, given by

$$P_{\mathcal{B}^2_{\mathbf{v},\epsilon}}(\mathbf{x}) = \begin{cases} \mathbf{x}, & \text{if } \mathbf{x} \in \mathcal{B}^2_{\mathbf{v},\epsilon}, \\ \mathbf{v} + \frac{\varepsilon(\mathbf{x}-\mathbf{v})}{\|\mathbf{x}-\mathbf{v}\|_2}, & \text{otherwise.} \end{cases} \tag{7}$$

*2) Total Variation:* By letting $\mathbf{D}_v$ and $\mathbf{D}_h \in \mathbb{R}^{N\times N}$ be the vertical and horizontal first-order differential operators, respectively, with Neumann boundaries, the differential operator is expressed by $\mathbf{D} := [\mathbf{D}_v^\top\ \mathbf{D}_h^\top]^\top \ \left(\in \mathbb{R}^{2N\times N}\right)$ for a vectorized gray image with $N$ pixels, and thus the TV is defined as [21]–[23]

$$\|\mathbf{x}\|_{\mathrm{TV}} := \|\mathbf{D}\mathbf{x}\|_{1,2} = \sum_{i=1}^{N} \sqrt{(\mathbf{D}_v\mathbf{x})_i^2 + (\mathbf{D}_h\mathbf{x})_i^2}, \tag{8}$$

where $(\mathbf{D}_v\mathbf{x})_i$ and $(\mathbf{D}_h\mathbf{x})_i$ are the $i$-th element of $\mathbf{D}_v\mathbf{x}$ and $\mathbf{D}_h\mathbf{x}$, respectively.

The minimization problem with TV regularization, which is often used in PnP-ADMM as denoiser, is defined as

$$\mathbf{x}^\star = \arg\min_{\mathbf{x}} \|\mathbf{x}\|_{\mathrm{TV}} + \frac{\lambda}{2}\|\mathbf{x} - \mathbf{x}_{\mathrm{in}}\|_2^2, \tag{9}$$

where $\mathbf{x}_{\mathrm{in}}$ is a vectorized input image and $\lambda > 0$ is a balancing weight of two terms.

## III. Proposed Method

### A. Data Model

Let $\mathbf{x}_m \in \mathbb{R}^N (m = 1, \ldots, M+1)$ be vectorized frames of a latent video, where $N$ is the number of pixels and $M+1$ is the number of frames. Let $\mathbf{y}_m \in \mathbb{R}^N (m = 1, \ldots, M+1)$ be vectorized observed frames, we consider the following observation model

$$\mathbf{y}_m = \mathbf{x}_m + \mathbf{n}_m. \tag{10}$$

where $\mathbf{n}_m \in \mathbb{R}^N$ is AWGN.

[1] Let $\mathbf{x} \in \mathbb{R}^N$ be an input vector. For a given non-empty closed convex set $\mathcal{C}$, the indicator function of $\mathcal{C}$ is defined by $\iota_C(\mathbf{x})$, which returns 0 if $\mathbf{x} \in \mathcal{C}$, and $+\infty$ otherwise.

**Algorithm 1** Proposed algorithm for (15)

**Input** : $\mathbf{Y}$, $\mathbf{Z}_i^{(0)}$, $\mathbf{\Theta}_i^{(0)}, \gamma_i\ (i=1,2,3)$, $\alpha$, $\epsilon$
**Output** : $\mathbf{\Phi}^{(t)}$
**while** A stopping criterion is not satisfied **do**
  $\mathbf{\Phi}^{(t+1)} \leftarrow \arg\min_{\mathbf{\Phi}} \frac{\gamma_1}{2}\|\mathbf{Z}_1^{(t)} - \mathbf{\Phi B \Sigma} - \mathbf{\Theta}_1^{(t)}\|_F^2 + \frac{\gamma_2}{2}\|\mathbf{Z}_2^{(t)} - \mathbf{\Phi} - \mathbf{\Theta}_2^{(t)}\|_F^2 + \frac{\gamma_3}{2}\|\mathbf{Z}_3^{(t)} - \mathbf{\Phi B \Sigma} - \mathbf{\Theta}_3^{(t)}\|_F^2$;
  $\mathbf{Z}_1^{(t+1)} \leftarrow \mathcal{D}_{\mathcal{R}_r, \alpha/\gamma_1}\left(\mathbf{\Phi}^{(t+1)}\mathbf{B\Sigma} + \mathbf{\Theta}_1^{(t)}\right)$;
  $\mathbf{Z}_2^{(t+1)} \leftarrow \mathcal{D}_{\mathcal{R}_m, (1-\alpha)/\gamma_2}\left(\mathbf{\Phi}^{(t+1)} + \mathbf{\Theta}_2^{(t)}\right)$;
  $\mathbf{Z}_3^{(t+1)} \leftarrow P_{\mathcal{B}^F_{\mathbf{Y},\epsilon}}\left(\mathbf{\Phi}^{(t+1)}\mathbf{B\Sigma} + \mathbf{\Theta}_3^{(t)}\right)$;
  $\mathbf{\Theta}_1^{(t+1)} \leftarrow \mathbf{\Theta}_1^{(t)} + \mathbf{\Phi}^{(t+1)}\mathbf{B\Sigma} - \mathbf{Z}_1^{(t+1)}$;
  $\mathbf{\Theta}_2^{(t+1)} \leftarrow \mathbf{\Theta}_2^{(t)} + \mathbf{\Phi}^{(t+1)} - \mathbf{Z}_2^{(t+1)}$;
  $\mathbf{\Theta}_3^{(t+1)} \leftarrow \mathbf{\Theta}_3^{(t)} + \mathbf{\Phi}^{(t+1)}\mathbf{B\Sigma} - \mathbf{Z}_3^{(t+1)}$;
  $t \leftarrow t+1$;
**end while**

Therefore, we defined the matrix form of $m = 1, \ldots, M$ frames of the observed video and decomposed it by the DMD algorithm described in Section II-A as

$$\mathbf{Y} := [\mathbf{y}_1\ \mathbf{y}_2\ \ldots\ \mathbf{y}_M] \approx \widehat{\mathbf{\Phi}}\mathbf{B\Sigma}. \tag{11}$$

where $\widehat{\mathbf{\Phi}} \in \mathbb{C}^{N\times r}$ is the matrix of the noisy DMD mode. We assumed that the DMD mode only degraded, and then, their amplitudes $\mathbf{B}$ and the temporal evolution $\mathbf{\Sigma}$ are hardly affected by noise.

### B. Minimization Problem

Our aim is to find the noiseless DMD mode $\mathbf{\Phi}^*$ from a noisy observed video $\mathbf{Y} \approx \widehat{\mathbf{\Phi}}\mathbf{B\Sigma}$. The proposed minimization problem for the noiseless DMD mode estimation is defined by

$$\begin{aligned} &\min_{\mathbf{\Phi}} \alpha\mathcal{R}_r(\mathbf{\Phi B\Sigma}) + (1-\alpha)\mathcal{R}_m(\mathbf{\Phi}) \\ &\text{s.t. } \|\mathbf{Y} - \mathbf{\Phi B \Sigma}\|_F \le \epsilon \end{aligned} \tag{12}$$

where $\mathcal{R}_r$ and $\mathcal{R}_m$ are regularization terms for a reconstruct video $\mathbf{\Phi B\Sigma}$ and the DMD mode $\mathbf{\Phi}$, respectively, and $\alpha \in [0,1]$ is the balancing weight of these terms. Based on the Plug-and-Play framework, the proposed minimization problem simultaneously reduces the Gaussian noise of the reconstruct video and the DMD mode under the Frobenius-reconstruction error constraint with $\epsilon$ and Gaussian denoiser associated with $\mathcal{R}_r$ and $\mathcal{R}_m$.

To find a solution of (12), we use PnP-ADMM described in Section II-B.

### C. Optimization

We define the convex set $\mathcal{B}^F_{\mathbf{Y},\epsilon}$ similar to (7) as

$$\mathcal{B}^F_{\mathbf{Y},\epsilon} := \left\{\mathbf{X} \in \mathbb{R}^{N\times M} \mid \|\mathbf{Y} - \mathbf{X}\|_F \le \epsilon\right\}. \tag{13}$$

To apply PnP-ADMM, we first reformulate (12) into the following unconstrained problem

$$\min_{\mathbf{\Phi}} \alpha\mathcal{R}_r(\mathbf{\Phi B\Sigma}) + (1-\alpha)\mathcal{R}_m(\mathbf{\Phi}) + \iota_{\mathcal{B}^F_{\mathbf{Y},\epsilon}}(\mathbf{\Phi B\Sigma}), \tag{14}$$

where $\iota_{\mathcal{B}^F_{\mathbf{Y},\epsilon}}(\cdot)$ is the indicator function of $\mathcal{B}^F_{\mathbf{Y},\epsilon}$. This function guarantees that the Frobenius norm of $\mathbf{Y} - \mathbf{\Phi B\Sigma}$ is less than or equal to $\epsilon$. Thus, the role of the third term of (14) corresponds to the role of the constraint of (12) in minimization.

By introducing auxiliary variables $\mathbf{Z}_1 \in \mathbb{C}^{N\times M}, \mathbf{Z}_2 \in \mathbb{C}^{N\times r}$, and $\mathbf{Z}_3 \in \mathbb{C}^{N\times M}$, we rewrite the minimization problem (14) into the following equivalent expression:

$$\begin{aligned} &\min_{\mathbf{\Phi}, \mathbf{Z}_i (i=1,2,3)} \alpha\mathcal{R}_r(\mathbf{Z}_1) + (1-\alpha)\mathcal{R}_m(\mathbf{Z}_2) + \iota_{\mathcal{B}^F_{\mathbf{Y},\epsilon}}(\mathbf{Z}_3), \\ &\text{s.t. } \mathbf{Z}_1 = \mathbf{\Phi B\Sigma}, \mathbf{Z}_2 = \mathbf{\Phi}, \mathbf{Z}_3 = \mathbf{\Phi B\Sigma}. \end{aligned} \tag{15}$$

The algorithm for solving (15) with $\gamma_i\ (i=1,2,3)$ is summarized in Algorithm 1.

The update of $\mathbf{\Phi}$ is achieved by solving a simple quadratic minimization problem.

In the proposed algorithm, the solution of the sub-problems w.r.t. $\mathbf{Z}_1$ and $\mathbf{Z}_2$ are replaced by the Gaussian denoiser, respectively, to yield

$$\mathbf{Z}_1^{(t+1)} = \mathcal{D}_{\mathcal{R}_r, \alpha/\gamma_1}\left(\mathbf{\Phi}^{(t+1)}\mathbf{B\Sigma} + \mathbf{\Theta}_1^{(t)}\right), \tag{16}$$

$$\mathbf{Z}_2^{(t+1)} = \mathcal{D}_{\mathcal{R}_m, (1-\alpha)/\gamma_2}\left(\mathbf{\Phi}^{(t+1)} + \mathbf{\Theta}_2^{(t)}\right). \tag{17}$$

In our experiments, we used the total variation minimization method described in Section II-B2 for both denoiser $\mathcal{D}_{\mathcal{R}_r, \alpha/\gamma_1}$ and $\mathcal{D}_{\mathcal{R}_m, (1-\alpha)/\gamma_2}$. Thus, minimizing the proposed problem with the TV denoiser yields a set of spatially smooth DMD modes that can reconstruct spatially smooth frames.

The solution of the sub-problems w.r.t. $\mathbf{Z}_3$ is computed by Frobenius norm ball projection $P_{\mathcal{B}^F_{\mathbf{Y},\epsilon}}$ that is similar to (7).

## IV. Experiments

To demonstrate the effectiveness of the proposed method, we applied our method to noisy videos[2], each of which has $M = 19$ frames, artificially degraded by AWGN with five types of intensities and compared it with the conventional TV method. Furthermore, the results of the proposed method in the case of $\alpha = 0$ were also presented, that is, this method only considers the spatial smoothness of each DMD mode. For the quality metrics, we used PSNR and SSIM [25]. For the parameter setting of the proposed method, we set $\epsilon = 0.95\sqrt{NM}\sigma$ and found the visually best results by adjusting the value of $\alpha$ from 0 to 1 in increments of 0.1. For the TV method, we found the visually best results by adjusting $\lambda$.

The averaged PSNR and SSIM values are shown in Table I and II, respectively. We calculated PSNR and SSIM for each frame of each video, and compared its average values. In the case of Ours, the values of $\alpha$ that gave the best results are shown in parentheses. One can observe from both tables that our method, which regularizes both the DMD mode and the reconstructed video, has the highest values compared with the TV method and the method that regularizes only the DMD mode.

Figure 1 shows some closeups of the 19th frame of Scene 1 and Scene 2 degraded by AWGN with the standard deviation $\sigma = 25/255$. One can observe from the figure that our method effectively removes noise compared with the other methods. Although the TV method produces smooth images,

[2]We used the SBMnet dataset [24]. For the sake of simplicity, a color video was converted to a grayscale video and used in our experiment.

Fig. 1. Results of the 19th frame in Scene 1 (top) and Scene 2 (bottom) : (from left to right) reference frame, noisy frame, TV result, Ours with $\alpha = 0$, and Ours.

TABLE I
PSNR COMPARISON.

| Scene | $\sigma$ | Noisy | TV | Ours with $\alpha = 0$ | Ours ($\alpha$) |
|---|---|---|---|---|---|
| 1 | 15/255 | 24.76 | 31.99 | 27.28 | **32.92** (0.1) |
| | 20/255 | 22.32 | 30.37 | 24.47 | **31.14** (0.2) |
| | 25/255 | 20.44 | 29.06 | 22.13 | **29.83** (0.2) |
| | 30/255 | 18.92 | 27.88 | 20.00 | **28.70** (0.3) |
| | 35/255 | 17.65 | 26.78 | 18.48 | **27.66** (0.4) |
| 2 | 15/255 | 24.75 | 26.92 | 26.50 | **28.38** (0.1) |
| | 20/255 | 22.30 | 25.33 | 24.04 | **26.56** (0.1) |
| | 25/255 | 20.43 | 24.14 | 21.99 | **25.33** (0.2) |
| | 30/255 | 18.92 | 23.18 | 20.01 | **24.34** (0.2) |
| | 35/255 | 17.66 | 22.35 | 18.53 | **23.42** (0.3) |
| 3 | 15/255 | 24.64 | 31.20 | 26.43 | **31.94** (0.2) |
| | 20/255 | 22.16 | 29.92 | 23.73 | **30.50** (0.3) |
| | 25/255 | 20.26 | 28.94 | 21.47 | **29.47** (0.3) |
| | 30/255 | 18.71 | 28.13 | 19.76 | **28.57** (0.4) |
| | 35/255 | 17.43 | 27.40 | 18.18 | **27.82** (0.5) |

TABLE II
SSIM COMPARISON.

| Scene | $\sigma$ | Noisy | TV | Ours with $\alpha = 0$ | Ours ($\alpha$) |
|---|---|---|---|---|---|
| 1 | 15/255 | 0.4542 | 0.8883 | 0.5673 | **0.8969** (0.2) |
| | 20/255 | 0.3573 | 0.8637 | 0.4480 | **0.8717** (0.3) |
| | 25/255 | 0.2915 | 0.8404 | 0.3564 | **0.8492** (0.3) |
| | 30/255 | 0.2439 | 0.8167 | 0.2802 | **0.8212** (0.4) |
| | 35/255 | 0.2080 | 0.7920 | 0.2329 | **0.8027** (0.5) |
| 2 | 15/255 | 0.7679 | 0.8555 | 0.8206 | **0.8919** (0.1) |
| | 20/255 | 0.6809 | 0.8025 | 0.7428 | **0.8441** (0.2) |
| | 25/255 | 0.6043 | 0.7525 | 0.6666 | **0.8113** (0.2) |
| | 30/255 | 0.5382 | 0.7046 | 0.5850 | **0.7745** (0.2) |
| | 35/255 | 0.4814 | 0.6579 | 0.5196 | **0.7338** (0.3) |
| 3 | 15/255 | 0.4948 | 0.8438 | 0.5772 | **0.8607** (0.2) |
| | 20/255 | 0.3832 | 0.8099 | 0.4550 | **0.8260** (0.3) |
| | 25/255 | 0.3054 | 0.7810 | 0.3573 | **0.7955** (0.4) |
| | 30/255 | 0.2493 | 0.7559 | 0.2906 | **0.7699** (0.4) |
| | 35/255 | 0.2079 | 0.7330 | 0.2343 | **0.7478** (0.5) |

the contours of the people and the textures of the floor and trees are not well preserved compared with our method. When the regularization weight of the proposed method is set to $\alpha = 0$, i.e., the total variation of the DMD mode is only minimized, the noise is not sufficiently removed in the image domain because the smoothness of the image domain is not taken into account.

Figure 2 shows an example of dynamic modes $\phi_1, \phi_5$, and $\phi_{15}$ in Scene 1 degraded by AWGN with the standard deviation $\sigma = 25/255$. From this figure, one observes that the proposed method can remove noise in each mode while preserving the dynamic mode of the scene.

## V. CONCLUSIONS

In this paper, we introduced a novel noise removal method for the DMD mode of a noisy video. The minimization problem that simultaneously reduces the noise of the DMD mode and the reconstructed video was defined. We solved the proposed minimization problem by using the proposed algorithm based on PnP-ADMM. Experiments confirmed that the proposed method can efficiently remove noise on the DMD mode and the reconstructed video.

In future works, we will attempt to improve the computational efficiency of the proposed PnP-ADMM algorithm by employing stochastic gradient descent algorithms, and we will apply the proposed scheme for other high-dimensional volume data denoising problems, e.g., hyperspectral imaing and CT/MRI imaging.

## ACKNOWLEDGMENT

This work was partially supported by JSPS KAKENHI Grant Number 21K17767.

## REFERENCES

[1] J. Grosek and J. Kutz, "Dynamic mode decomposition for real-time background/foreground separation in video," *ArXiv*, vol. abs/1404.7592, 2014.

[2] J. N. Kutz, J. Grosek, and S. L. Brunton, "Dynamic mode decomposition for robust pca with applications to foreground/background subtraction in video streams and multi-resolution analysis," *CRC Handbook on Robust Low-Rank and Sparse Matrix Decomposition: Applications in Image and Video Processing*, 2016.

[3] N. B. Erichson and C. Donovan, "Randomized low-rank dynamic mode decomposition for motion detection," *Computer Vision and Image Understanding*, vol. 146, pp. 40–50, 2016.

[4] N. B. Erichson, S. L. Brunton, and J. N. Kutz, "Compressed dynamic mode decomposition for background modeling," *Journal of Real-Time Image Processing*, vol. 16, no. 5, pp. 1479–1492, 2019.

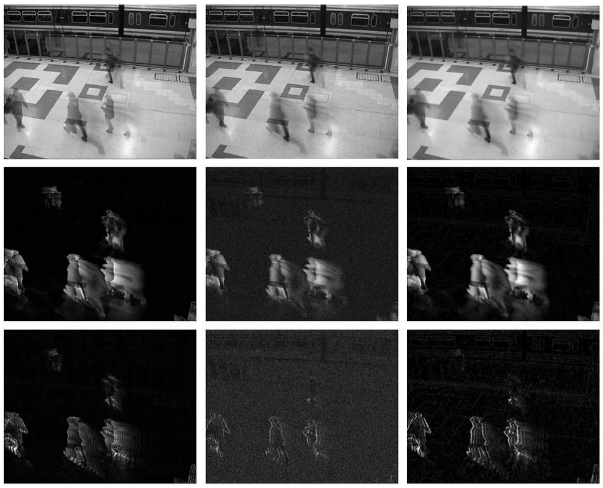

Fig. 2. Example of dynamic modes (top to bottom) $\phi_1, \phi_5$, and $\phi_{15}$ in Scene 1 : (from left to right) ground truth, noisy, and Ours.


[5] J. N. Kutz, X. Fu, S. L. Brunton, and N. B. Erichson, "Multi-resolution dynamic mode decomposition for foreground/background separation and object tracking," in *2015 IEEE International Conference on Computer Vision Workshop (ICCVW)*, 2015, pp. 921–929.

[6] P. J. SCHMID, "Dynamic mode decomposition of numerical and experimental data," *Journal of Fluid Mechanics*, vol. 656, p. 5–28, 2010.

[7] I. Mezić, "Analysis of fluid flows via spectral properties of the koopman operator," *Annual Review of Fluid Mechanics*, vol. 45, no. 1, pp. 357–378, 2013. [Online]. Available: https://doi.org/10.1146/annurev-fluid-011212-140652

[8] J. N. Kutz, S. L. Brunton, B. W. Brunton, and J. L. Proctor, *Dynamic Mode Decomposition*. Philadelphia, PA: Society for Industrial and Applied Mathematics, 2016. [Online]. Available: https://epubs.siam.org/doi/abs/10.1137/1.9781611974508

[9] S. T. Dawson, M. S. Hemati, M. O. Williams, and C. W. Rowley, "Characterizing and correcting for the effect of sensor noise in the dynamic mode decomposition," *Experiments in Fluids*, vol. 57, no. 3, p. 42, 2016.

[10] M. S. Hemati, C. W. Rowley, E. A. Deem, and L. N. Cattafesta, "De-biasing the dynamic mode decomposition for applied koopman spectral analysis of noisy datasets," *Theoretical and Computational Fluid Dynamics*, vol. 31, no. 4, pp. 349–368, 2017.

[11] L. I. Rudin, S. Osher, and E. Fatemi, "Nonlinear total variation based noise removal algorithms," *Phys. D*, vol. 60, no. 1-4, pp. 259–268, 1992.

[12] X. Bresson and T. F. Chan, "Fast dual minimization of the vectorial total variation norm and applications to color image processing," *Inverse Probl. Imag.*, vol. 2, no. 4, pp. 455–484, 2008.

[13] A. Chambolle, "An algorithm for total variation minimization and applications," *J. Math. Imaging Vis.*, vol. 20, no. 1-2, pp. 89–97, 2004.

[14] P. Blomgren and T. F. Chan, "Color tv: total variation methods for restoration of vector-valued images," *IEEE Trans. Image Process.*, vol. 7, no. 3, pp. 304–309, 1998.

[15] K. Dabov, A. Foi, and K. Egiazarian, "Video denoising by sparse 3d transform-domain collaborative filtering," in *2007 15th European Signal Processing Conference*, Sept 2007, pp. 145–149.

[16] J. H. Tu, "Dynamic mode decomposition: Theory and applications," Ph.D. dissertation, Princeton University, 2013.

[17] S. L. Brunton, J. L. Proctor, J. H. Tu, and J. N. Kutz, "Compressed sensing and dynamic mode decomposition," *Journal of Computational Dynamics*, vol. 2, no. 2, p. 165, 2015.

[18] D. Gabay and B. Mercier, "A dual algorithm for the solution of nonlinear variational problems via finite element approximation," *Comput. & Math. Appl.*, vol. 2, no. 1, pp. 17 – 40, 1976.

[19] S. V. Venkatakrishnan, C. A. Bouman, and B. Wohlberg, "Plug-and-play priors for model based reconstruction," in *2013 IEEE Global Conference on Signal and Information Processing*. IEEE, 2013, pp. 945–948.

[20] S. H. Chan, X. Wang, and O. A. Elgendy, "Plug-and-play admm for image restoration: Fixed-point convergence and applications," *IEEE Transactions on Computational Imaging*, vol. 3, no. 1, pp. 84–98, 2016.

[21] X. Bresson and T. F. Chan, "Fast dual minimization of the vectorial total variation norm and applications to color image processing," *Inverse Probl. Imag.*, vol. 2, no. 4, pp. 455–484, 2008.

[22] P. L. Combettes and J.-C. Pesquet, "A proximal decomposition method for solving convex variational inverse problems," *Inverse Probl.*, vol. 24, no. 6, p. 065014, 2008.

[23] V. Duval, J.-F. Aujol, and L. A. Vese, "Mathematical modeling of textures: Application to color image decomposition with a projected gradient algorithm," *J. Math. Imag. Vis.*, vol. 37, no. 3, pp. 232–248, 2010.

[24] P.-M. Jodoin, L. Maddalena, A. Petrosino, and Y. Wang, "Extensive benchmark and survey of modeling methods for scene background initialization," *IEEE Transactions on Image Processing*, vol. 26, no. 11, pp. 5244–5256, 2017.

[25] Z. Wang, A. Bovik, H. Sheikh, and E. Simoncelli, "Image quality assessment: from error visibility to structural similarity," *IEEE Trans. Image Process.*, vol. 13, no. 4, pp. 600–612, 2004.